Supplementary Information

Characterizing airborne nanoparticles in six Chinese cities based on their interactions with natural air ions

Jin Wu[1], Hao Wu[1], Yiran Li[1], Tingyu Liu[2], Mei Zheng[3], Cheng Huang[4,5], Fang Zhang[6], Jun Zhao[7], Jianwu Shi[8], Xiaoxiao Li[9], Yongchun Liu[2], Rujing Yin[10], Xiaotong Chen[11], Qiang Zhang[1], Jiming Hao[1], Jingkun Jiang[1,*]

[1]State Key Joint Laboratory of Environment Simulation and Pollution Control, School of Environment, Tsinghua University, Beijing, 100084, China

[2]Aerosol and Haze Laboratory, Beijing Advanced Innovation Center for Soft Matter Science and Engineering, Beijing University of Chemical Technology, 100029 Beijing, China

[3]State Key Joint Laboratory of Environmental Simulation and Pollution Control, College of Environmental Sciences and Engineering, Peking University, Beijing, 100871, China

[4]State Environmental Protection Key Laboratory of Formation and Prevention of the Urban Air Pollution Complex, Shanghai Academy of Environmental Sciences, Shanghai, 200233, China

[5]Shanghai Environmental Monitoring Center, Shanghai, 200235, China

[6]School of Civil and Environmental Engineering, Harbin Institute of Technology (Shenzhen), Shenzhen, China

[7]School of Atmospheric Sciences, Guangdong Province Key Laboratory for Climate Change and Natural Disaster Studies, and Southern Marine Science and Engineering Guangdong Laboratory (Zhuhai), Sun Yat-sen University, Zhuhai, Guangdong, 519082, China

[8]Faculty of Environmental Science and Engineering, Kunming University of Science and Technology, Kunming, 650500, China

[9]School of Resource and Environmental Sciences, Wuhan University, Wuhan, 430072, China

[10]Key Laboratory of Industrial Ecology and Environmental Engineering (Ministry of Education), School of Environmental Science and Technology, Dalian University of Technology, 116024, Dalian, China

[11]Environmental Technology Division, Institute of Nuclear and New Energy Technology, Tsinghua University, Beijing, 100084, China

Correspondence to: Jingkun Jiang (jiangjk@tsinghua.edu.cn)

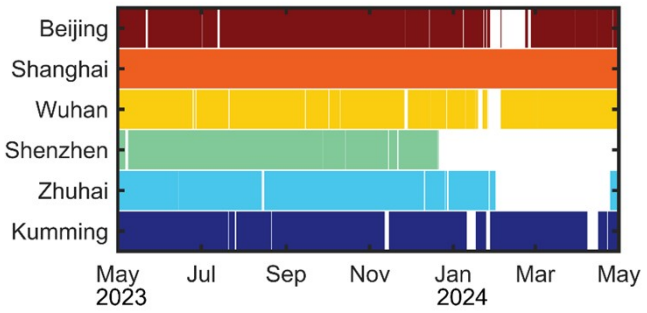

Figure S1. Data coverage of six sites. The colored areas represent valid data. Blank areas indicate the presence of invalid data.

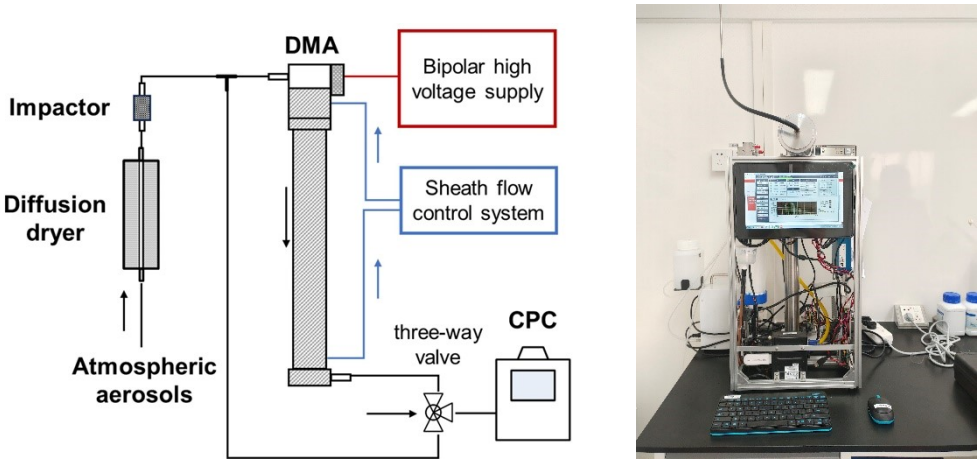

Figure S2. Schematic diagram[1] and photo of bipolar SMPS

Ambient air was sampled from the windows in Beijing, Wuhan and Kunming, and from rooftops in Shanghai, Shenzhen and Zhuhai. The sampling system of each site consists of a 1/4 in. stainless steel tubing, a diffusion dryer, and an impactor with a 50% cutting-off diameter of 2.5 μm. The length of sampling tube varies from sites, and we considered particle loss through the sampling tube during data inversion. The diffusion dryer is used to condition the relative humidity to be less than 40%. The $PM_{2.5}$ impactor is used to remove coarse particles.

For the DMA, we use a long DMA (Model 3081, TSI Corp.) and five home-built DMAs (Model Q-DMA-L, Beijing NaKe Environmental Technologies Co., Ltd). Figure S3a shows the profile chart of Q-DMA-L. Its inner radius is 0.937 cm, outer radius is 2.005 cm, and length is 44.369 cm. It has an annular aerosol flow distributor with small holes in the aerosol inlet zone. Then the aerosol flow is introduced to the classification region, moving downwards together with clean laminar sheath. Their sheath flow rate, size accuracy, and transfer function have been calibrated in the laboratory.

For the CPC, we use six CPCs (Model C003, Beijing NaKe Environmental Technologies Co., Ltd) with a nominal d_{p50} of 10 nm.[2] The butanol-based CPC operates at a flow rate of 0.3 $L \cdot min^{-1}$. The temperature of saturator, condenser and optical detector are set as 39 ℃, 18 ℃ and 40 ℃. In the saturator, the butanol evaporates, then it enters the condensation chamber together with aerosols. In the condenser, the supersaturated butanol condenses on the surface of aerosols. Aerosols grow to micro sizes and can be counted by the optical detector. Their counting efficiency for small particles varies with particle size due to the Kelvin effect, eventually stabilizing at a plateau value. Their counting efficiency have been calibrated against an electrometer (Model 3068B, TSI Corp.) to ensure the 50% efficiency diameter is 10 nm±1 nm and the plateau efficiency is 100% ± 5%.

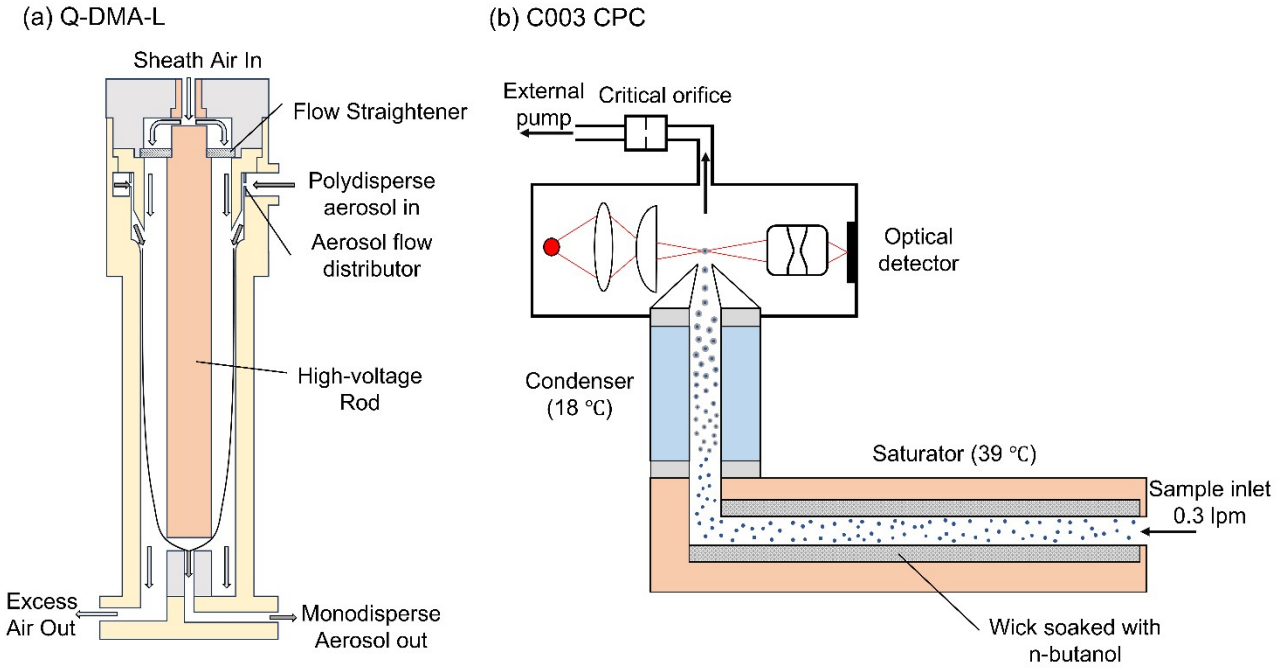

Figure S3. Schematic of the (a) Q-DMA-L and (b) C003 CPC

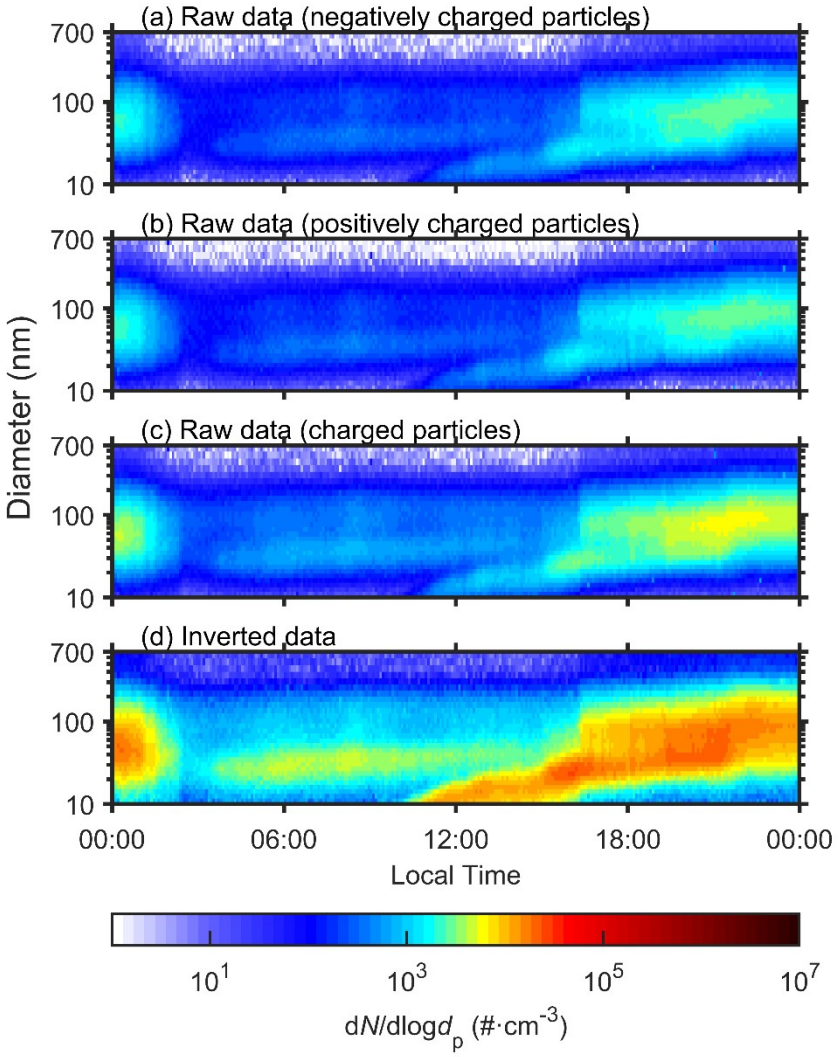

Figure S4. Example of raw data and inverted data

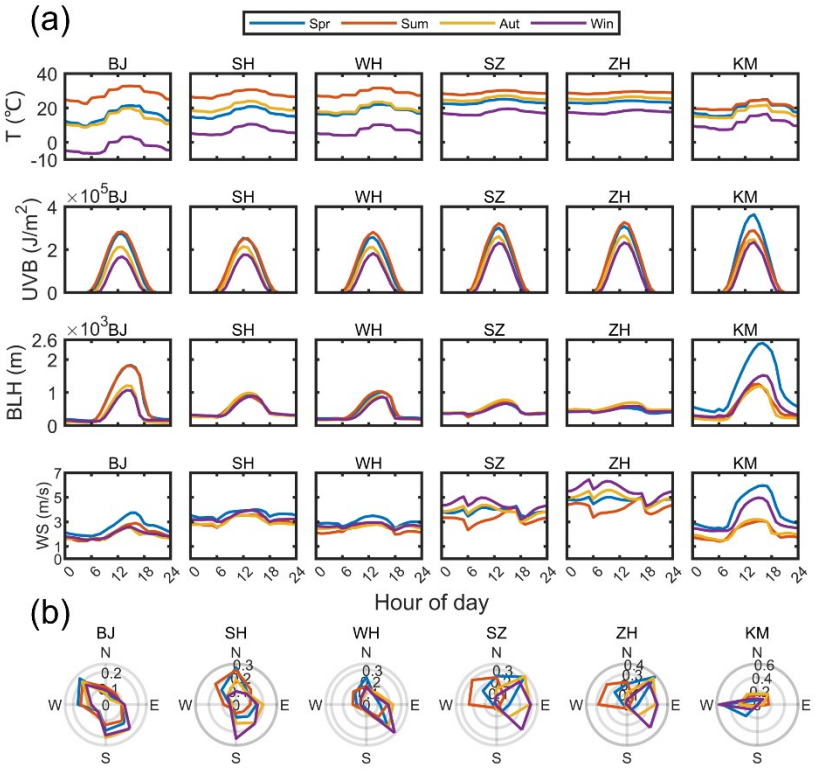

Figure S5. Meteorological data of six sites in 2023. Temperature (T), boundary layer height (BLH), UVB, wind speed (WS), and wind direction are extracted from grid data of the fifth generation ECMWF reanalysis (ERA5).[3]

A typical NPF day is characterized by two features: (1) a burst in the nucleation mode particle number concentration (< 25 nm), and (2) subsequent growth of these newly formed particles lasts for several hours.[4]

The event shown in Fig. S6a is an example of NPF day.[4] When there is neither a burst of nucleation mode particles nor subsequent growth of newly formed particles, it was classified as a non-NPF day (e.g., Fig. S6b). If the burst of nucleation mode particles is not followed by further particle growth, the day is classified as an undefined day (e.g., Fig. S6c).[5]

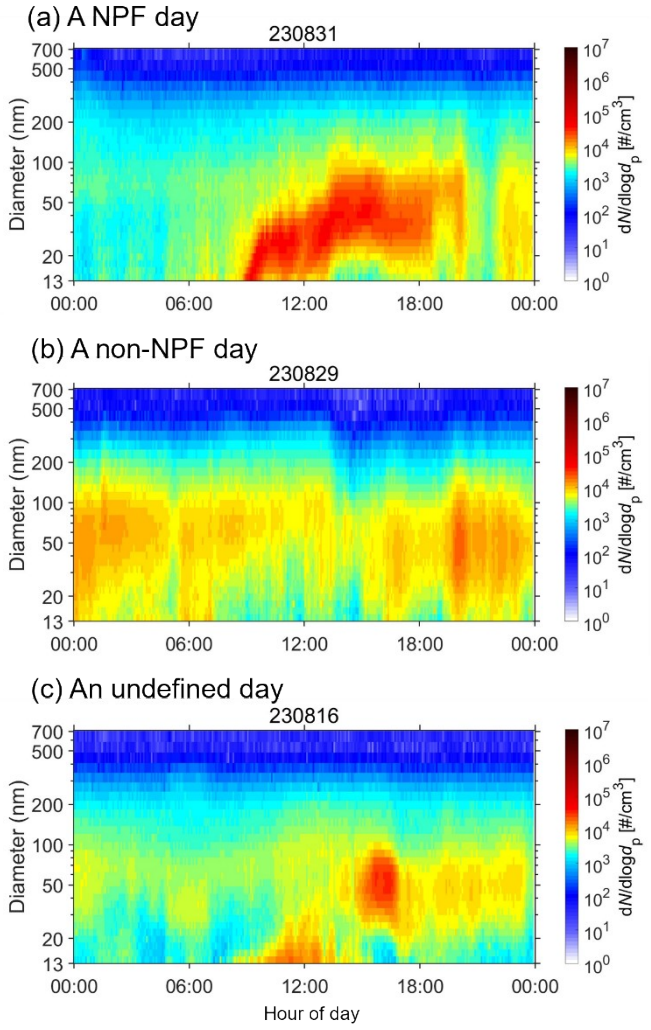

Figure S6. Examples of NPF, non-NPF and undefined days. The PNSD data is from Zhuhai site.

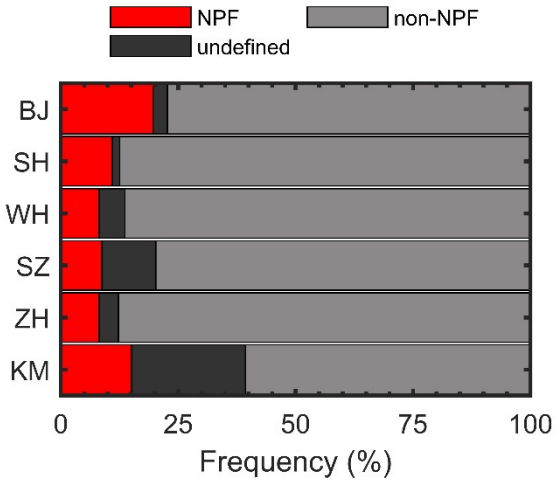

Figure S7. NPF frequency of six cities. The number of valid NPF/non-NPF days at each site are: 70/283 days (Beijing), 40/319 days (Shanghai), 30/316 days (Wuhan), 32/161 days (Shenzhen), 40/321 days (Zhuhai), 54/223 days (Kunming).

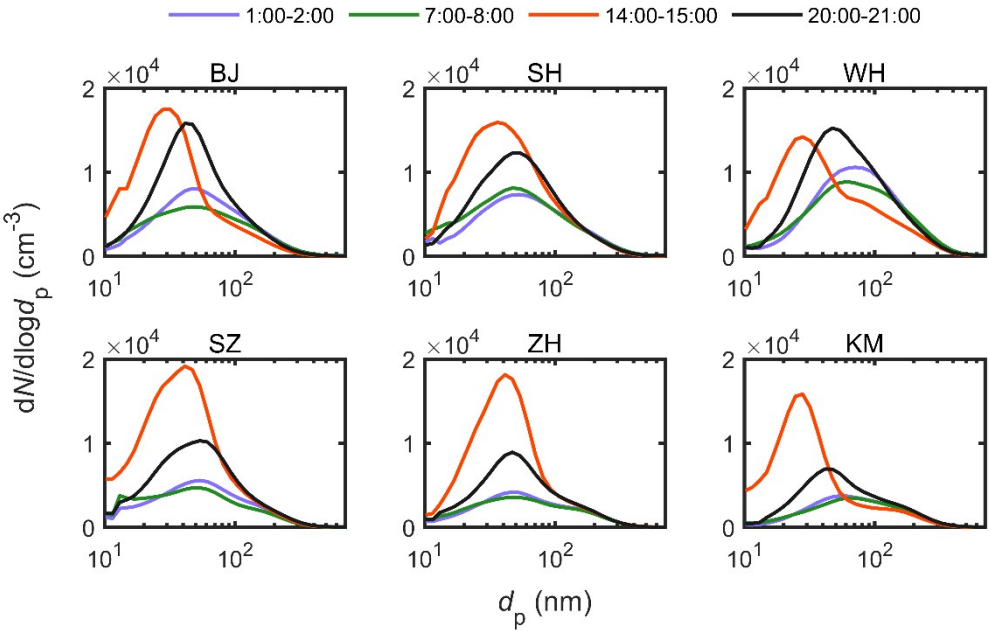

Figure S8. Mean PNSDs of NPF days.

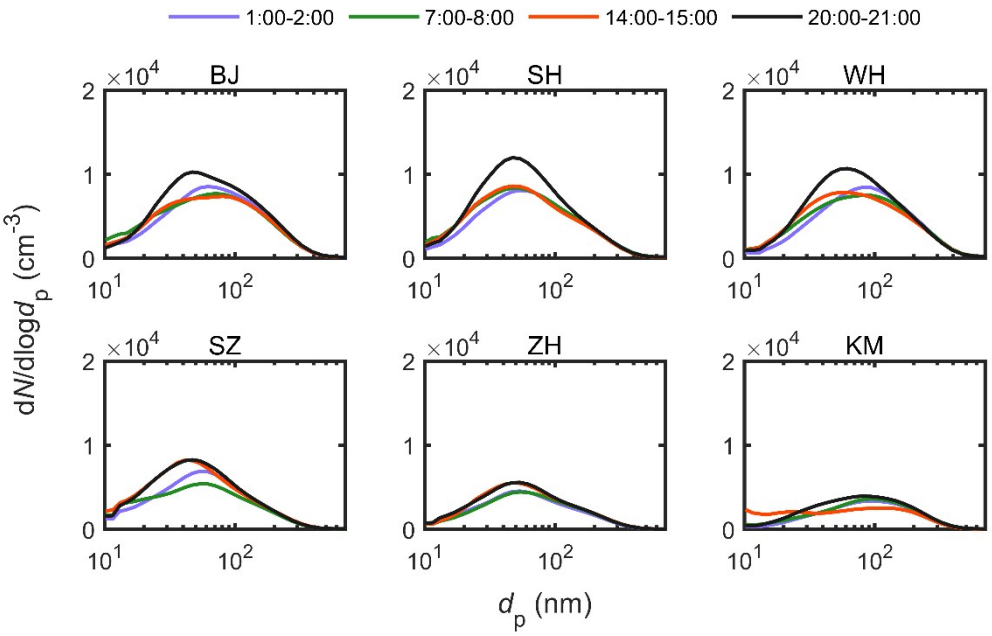

Figure S9. Mean PNSDs of non-NPF days.

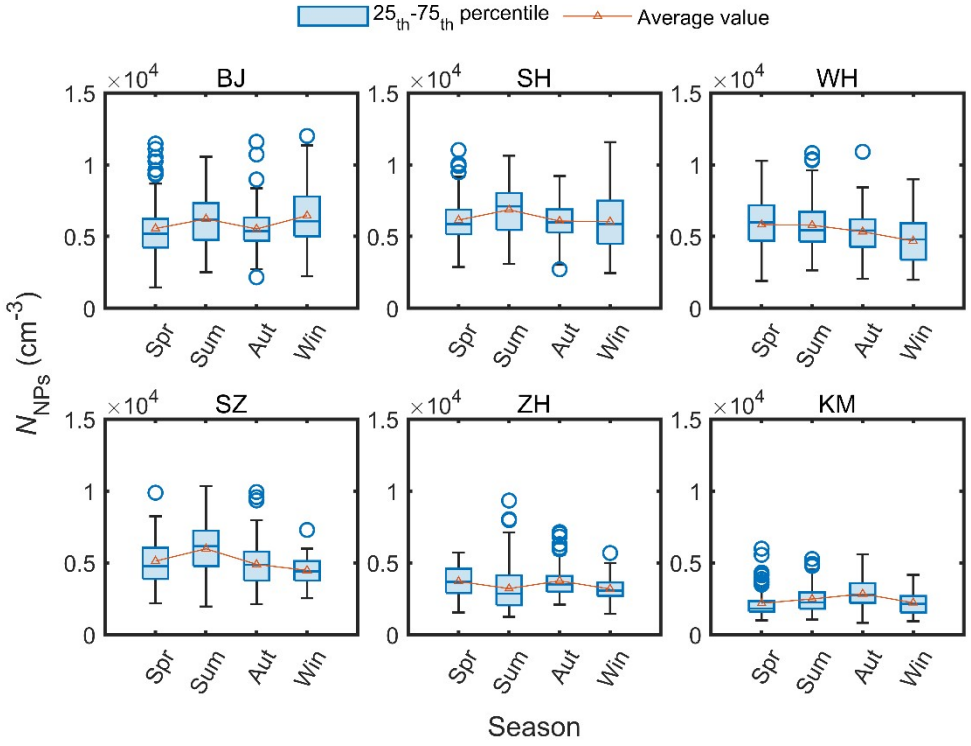

Figure S10. Seasonal variation of N_{NPs}

The measured PNSDs can be numerically fitted using a sum of n lognormal distribution functions,[6]

$$\frac{dN}{dlogd_p} = \sum_{i=1}^{n} \frac{N_i}{\sqrt{2\pi} log\sigma_i} exp\left[-\frac{(logd_p - log\bar{d}_{pi})}{2(log\sigma_i)^2} \right]$$

where N_i is the number concentration (cm^{-3}), $\bar{d}_{pi}$ is the median diameter (nm), σ_i is standard deviation of the ith lognormal mode. In this case, $3n$ parameters are needed to express a PNSD, and the least square method can be used to fit these parameters. To represent the observed PNSDs using functions, we fitted the observation results (Table S1 and Table S2).

Table S1. Lognormal fitting parameters for the mean PNSDs during NPF days at characteristic times.

Site	Time (UTC+8)	NPF days								
		Mode 1			Mode 2			Mode 3		
		$D_{p,1}$ nm	N_1 cm^{-3}	$\sigma_{g,1}$ □	$D_{p,2}$ nm	N_2 cm^{-3}	$\sigma_{g,2}$ □	$D_{p,3}$ nm	N_3 cm^{-3}	$\sigma_{g,3}$ □
Beijing	1:00-2:00	53.6	15415	2.2						□
	7:00-8:00	31.8	8459	2.01	99.6	5230	1.88			□
	14:00-15:00	22.4	17110	2.72	29.9	11138	1.47	121	1416	1.51
	20:00-21:00	41.7	6905	1.45	47.1	16489	2.18	142	529	1.38
Shanghai	1:00-2:00	54.8	15558	2.36						□
	7:00-8:00	11.1	947.1	1.33	49.6	17096	2.39			□
	14:00-15:00	32.6	23747	1.82	102	5867	1.81			□
	20:00-21:00	50.1	22519	2.14	□	□	□	□	□	□
Wuhan	1:00-2:00	3.53	7436	1.67	71.6	20110	2.08			□
	7:00-8:00	61.3	17143	2.26	157	1893	1.5			□
	14:00-15:00	26.5	18640	1.74	109	7115	1.82			□
	20:00-21:00	48.7	21854	1.82	144	4674	1.66	□	□	□
Shenzhen	1:00-2:00	17.6	2423	1.55	48.6	5793	1.59	127	3242	1.69
	7:00-8:00	13.7	374.6	1.05	41	10331	2.42	178	417	1.32
	14:00-15:00	2.4	29718	6	38.4	23450	1.72	157	1583	1.43
	20:00-21:00	47.7	19217	2.17	□	□	□	□	□	□
Zhuhai	1:00-2:00	49.7	7766	2.19	191	724.3	1.39			□
	7:00-8:00	45.6	7679	2.38	179	717.5	1.4			□
	14:00-15:00	33.5	17719	1.71	47.6	4669	1.32	132	3105	1.67
	20:00-21:00	21.5	3153	1.63	47.2	7452	1.48	120	3822	1.7
Kunming	1:00-2:00	64.6	6836	2.08	190	532.5	1.39			□
	7:00-8:00	40.3	2968	2.3	94.6	4227	1.93			□
	14:00-15:00	10.4	2476	1.32	27.3	15412	1.48	109	3516	1.78

	20:00-21:00	45.2	9457	1.77	159	2329	1.57	□	□	□

Table S2. Lognormal fitting parameters for the mean PNSDs during non-NPF days at characteristic times.

Site	Time (UTC+8)	non-NPF days								
		Mode 1			Mode 2			Mode 3		
		$D_{p,1}$ nm	N_1 cm^{-3}	$\sigma_{g,1}$ □	$D_{p,2}$ nm	N_2 cm^{-3}	$\sigma_{g,2}$ □	$D_{p,3}$ nm	N_3 cm^{-3}	$\sigma_{g,3}$ □
Beijing	1:00-2:00	36.3	7241	2.41	87.2	11562	2.03			
	7:00-8:00	38.2	12784	2.51	112	6602	1.85			
	14:00-15:00	49.6	15486	2.38	148	3138	1.59			
	20:00-21:00	52.2	19362	2.14	172	2991	1.57	□	□	□
Shanghai	1:00-2:00	59.3	17601	2.37						
	7:00-8:00	52.5	19536	2.51						
	14:00-15:00	49	18243	2.34	202	958.6	1.39			
	20:00-21:00	48.8	21316	2.05	186	2125	1.61	□	□	□
Wuhan	1:00-2:00	70.8	14990	2.23	149	2534	1.67			
	7:00-8:00	61.4	15497	2.4	162	2514	1.59			
	14:00-15:00	54.1	15304	2.19	179	3209	1.65			
	20:00-21:00	67.8	21919	2.24	□	□	□	□	□	□
Shenzhen	1:00-2:00	14	697.7	1.41	57.1	13199	2.19			
	7:00-8:00	17.4	3544	1.58	50.8	5590	1.62	127	3526	1.71
	14:00-15:00	43.3	16703	2.34	197	493.4	1.33			
	20:00-21:00	47.4	17161	2.32	□	□	□	□	□	□
Zhuhai	1:00-2:00	53.4	8894	2.25	202	400	1.34			
	7:00-8:00	56.6	8854	2.26	195	427.1	1.35			
	14:00-15:00	48	9660	2.02	179	1371	1.56			
	20:00-21:00	51.6	10795	2.22	206	485.7	1.36	□	□	□
Kunming	1:00-2:00	62	4560	2.21	145	2488	1.67			
	7:00-8:00	43.1	3390	2.42	123	4321	1.81			
	14:00-15:00	4.38	9562	1.52	27.9	5018	2.66	142	2821	1.7
	20:00-21:00	61.9	6999	2.22	161	1848	1.56	□	□	□

In Fig. 3a, the solid square and triangle of 2023 represent measurements by the bipolar SMPS network. The solid square in 2012 was a two-month average N_{NPs} measured by PSD at the Shanghai Academy of Environmental Science (SAES). The solid triangle points from 2020 to 2022 were the annual average values of N_{NPs} at the Beijing University of Chemical Technology (BUCT) site measured by us. The hollow square in 2013 was reported by Ling et al.[7] The hollow square in 2014 was estimated from winter measurement by Xiao et al.[8] The hollow triangles are reported by Shang et al.[9], which were measured continuously at Peking University (PKU), Beijing from 2013 to 2020.

Table S3. Details of Figure 3a

City	Station Name	Time	Instrumentation	Size Range of Instrument	Size range of nanoparticles (nm)	Reference
Beijing	Peking University (PKU)	Mar. 2004-Mar. 2006	TDMPS (charger+Hauke-type DMA+TSI 3025 CPC, charger+Hauke-type DMA+TSI 3010 CPC), TSI 3321 APS	3 nm-10μm	20-100	Wu et al., 2008[10]
		Jan. 2013-Dec. 2020	Kr85 charger+TSI 3085 DMA+TSI 3776 UCPC, Kr85 charger+TSI 3081 DMA+TSI 3776 UCPC	3 nm-700 nm	10-100	Shang et al., 2023[9]
		May. 2023-Apr. 2024	Bipolar SMPS (Q-DMA-L+C003 CPC）	10 nm-700 nm	10-100	This study
	Beijing University of Chemical Technology (BUCT)	Jan. 2020-Dec. 2022	DEG SMPS(Soft X-ray charger+mini-cy DMA+DEG CPC) , PSD (Soft X-ray charger+3081 DMA and 3085 DMA+3776 UCPC)	1.3 nm-10μm	10-100	This study
Shanghai	Fudan University (FDU)	Nov. 2013-Jan. 2014	Airmodus A11 PSM, charger+TSI 3085 DMA+TSI 3776 UCPC, charger+TSI 3081 DMA+3775 CPC	1.34 nm-615 nm	10-100	Xiao et al., 2015[8]
	Shanghai Academy of Environmental Sciences (SAES)	Oct.-Nov. 2012	PSD (Soft X-ray charger, 3081 DMA+3772CPC, 3085 DMA+3776 UCPC)	3 nm-10μm	10-100	This study
		Jan.-Dec. 2013	Soft X-ray charger+TSI 3081 DMA+TSI 3772 CPC , TSI 3221 APS	13.56 nm-736.5 nm	13.6-100	Ling et al., 2019[7]
		May. 2023-Apr. 2024	Bipolar SMPS (Q-DMA-L + C003 CPC）	10 nm-700 nm	10-100	This study

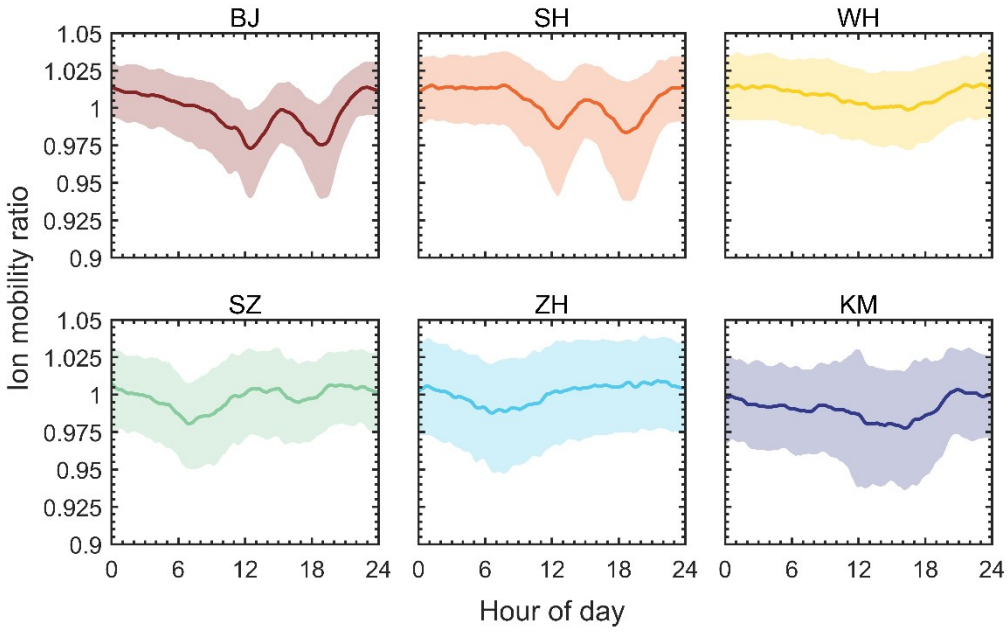

Figure S11. Diurnal cycles of ion mobility ratios at six sites, which are calculated by Equation (5). The lines are mean values of ion mobility ratio. The shaded areas represent the interquartile range (25th to 75th percentiles).

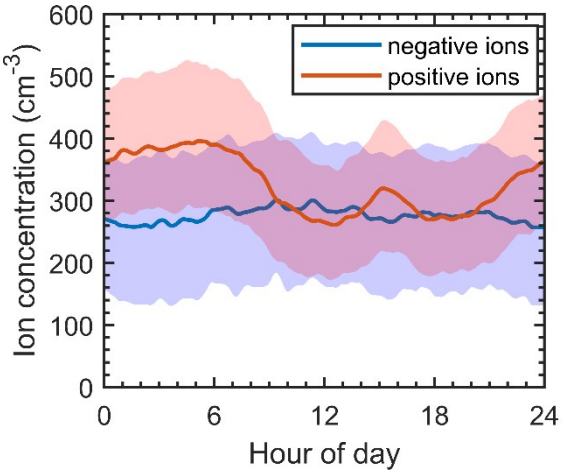

Figure S12. Concentration of cluster ions (3.2–0.5 $cm^2V^{-1}s^{-1}$, 0.8–1.6 nm) in Beijing. The lines are mean values of positive and negative ions. The shaded areas represent the interquartile range (25th to 75th percentiles).

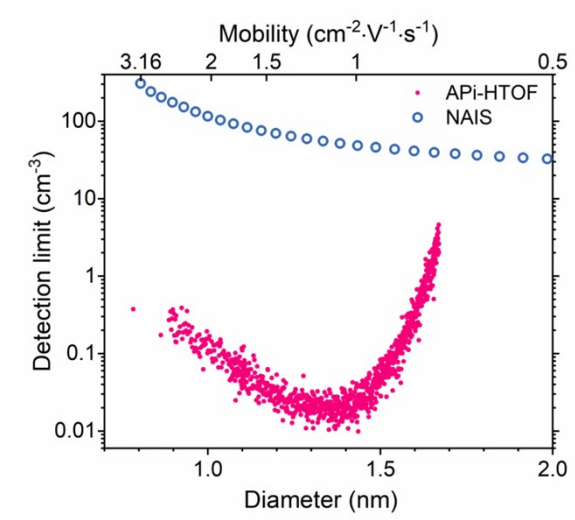

Figure S13. Detection limit of APi-TOF and NAIS

Reference

1. Y. Li, J. Wu, H. Wu, X. Liu, Q. Zhou, Y. Lu, Y. Wu, M. Liu, H. Ou, S. Mai, X. He, H. Song, H. Wang, P. Zeng, Y. Wang, D. Wang, Q. Zhang, J. Deng, J. Shi, X. Li, J. Zhao, F. Zhang, C. Huang, M. Zheng, J. Hao and J. Jiang, A bipolar SMPS network for measuring atmospheric aerosols using natural air ions, *Atmospheric Environment*, 2024, **325**, 120462.

2. Y. Li, X. Chen, J. Wu, Q. Zhang, Z. Zhang, J. Hao and J. Jiang, A convertible condensation particle counter using alcohol or water as the working fluid, *Aerosol Science and Technology*, 2024, DOI: 10.1080/02786826.2024.2395939, 1-10.

3. H. Hersbach, B. Bell, P. Berrisford, G. Biavati, A. Horányi, J. Muñoz Sabater, J. Nicolas, C. Peubey, R. Radu, I. Rozum, D. Schepers, A. Simmons, C. Soci, D. Dee and J.-N. Thépaut, ERA5 hourly data on single levels from 1940 to present.*Journal*, 2023, DOI: 10.24381/cds.adbb2d47.

4. M. Kulmala, T. Petaja, T. Nieminen, M. Sipila, H. E. Manninen, K. Lehtipalo, M. Dal Maso, P. P. Aalto, H. Junninen, P. Paasonen, I. Riipinen, K. E. Lehtinen, A. Laaksonen and V. M. Kerminen, Measurement of the nucleation of atmospheric aerosol particles, *Nat Protoc*, 2012, **7**, 1651-1667.

5. C. Deng, Y. Fu, L. Dada, C. Yan, R. Cai, D. Yang, Y. Zhou, R. Yin, Y. Lu, X. Li, X. Qiao, X. Fan, W. Nie, J. Kontkanen, J. Kangasluoma, B. Chu, A. Ding, V.-M. Kerminen, P. Paasonen, D. R. Worsnop, F. Bianchi, Y. Liu, J. Zheng, L. Wang, M. Kulmala and J. Jiang, Seasonal Characteristics of New Particle Formation and Growth in Urban Beijing, *Environ. Sci. Technol.*, 2020, **54**, 8547-8557.

6. J. H. Seinfeld and S. N. Pandis, *Atmospheric chemistry and physics: From air pollution to climate change*, John Wiley & Sons Third Edition edn., 2016.

7. Y. Ling, Y. Wang, J. Duan, X. Xie, Y. Liu, Y. Peng, L. Qiao, T. Cheng, S. Lou, H. Wang, X. Li and X. Xing, Long-term aerosol size distributions and the potential role of volatile organic compounds (VOCs) in new particle formation events in Shanghai, *Atmospheric Environment*, 2019, **202**, 345-356.

8. S. Xiao, M. Y. Wang, L. Yao, M. Kulmala, B. Zhou, X. Yang, J. M. Chen, D. F. Wang, Q. Y. Fu, D. R. Worsnop and L. Wang, Strong atmospheric new particle formation in winter in urban Shanghai, China, *Atmospheric Chemistry and Physics*, 2015, **15**, 1769-1781.

9. D. Shang, M. Hu, L. Tang, X. Fang, S. Chen, L. Zeng, S. Guo, Y. Zhang and Z. Wu, New Particle Formation Occurrence in the Urban Atmosphere of Beijing During 2013–2020, *Journal of Geophysical Research: Atmospheres*, 2023, **128**.

10. Z. Wu, M. Hu, P. Lin, S. Liu, B. Wehner and A. Wiedensohler, Particle number size distribution in the urban atmosphere of Beijing, China, *Atmospheric Environment*, 2008, **42**, 7967-7980.